

Performance Evaluation of an Enhanced Wideband CDMA Receiver using Channel Measurements¹

Karim Cheikhrouhou*, Sofiène Affes*, Ahmed Elderini*, Besma Smida*, Paul Mermelstein*,
Belhassen Sultana[†], and Venkatesh Sampath[‡]

*INRS-ÉMT, Université du Québec, Montreal, Canada - {cheikhro,affes,elderini,smida,mermel}@emt.inrs.ca

[†] Rogers Wireless, Montreal, Canada - Belhassen.Sultana@rci.rogers.com

[‡] OZ Communications Inc., Montreal, Canada - venkatesh.sampath@oz.com

Abstract—The spatio-temporal array-receiver (STAR) decomposes generic wideband CDMA channel responses across various parameter dimensions (*e.g.*, time-delays, multipath components, etc..) and extracts the associated time-varying parameters (*i.e.*, analysis) before reconstructing the channel (*i.e.*, synthesis) with increased accuracy. This work verifies the performance of STAR by comparing the results achieved with generic and measured channels for an average multipath power profile of [0, -4, -8] dB and a vehicular speed below 30 Km/h. The results suggest that losses due to operations with real 5 MHz channels are only 1 dB in SNR and 20-30% in capacity with DBPSK and single transmit and receive antennas. The corresponding SNR threshold for operation with real channels is about 5 dB.

I. INTRODUCTION

New technical results in transceiver design are expected to influence significantly the organization of future third-generation (3G) wireless networks and beyond (3G+) to support multimedia data communication and wireless access to the Internet. Yet the prospective innovative solutions that are most likely to make their shortest way to integration in a future real-world wireless system are those that take into account interaction with other subsystem components, any source of imperfection such as estimation and modeling errors, realistic link/system-level software simulation, off-line validation over channel measurements, and so forth to the proof-of-concept.

Motivated by the need for increased bandwidth efficiencies, we have recently developed a new spatio-temporal array-receiver (STAR) [1], [2] that achieves accurate and fast temporal synchronization, channel identification and efficient signal combining with significant gains in performance over RAKE-type receivers [2], [3]. More recently, we upgraded STAR to integrate space-time multi-user detection based on interference subspace rejection (ISR) [4], carrier frequency offset (CFO) recovery (CFOR) [5] and multiple-input multiple-output (MIMO) high-speed transmissions on the downlink [6]. All these significant enhancements exploit the powerful dynamic channel parameter extraction capabilities of STAR based on *a priori* known

generic models for these parameters. Indeed, STAR applies an “analysis/synthesis” principle where it decomposes the channel over various channel parameter dimensions (*e.g.*, time-delays, shaping pulse, Rayleigh fades, etc..), estimates those time-varying parameters (*i.e.*, analysis) then uses them to reconstruct the channel (*i.e.*, synthesis) with increased accuracy [1], [2], [4]. So far, these software developments were validated using generic channel models only. Verification of STAR’s performance [7] using real-world channel measurements is therefore an important step toward practical hardware implementation [8].

Along this perspective, we evaluate in this work the performance of STAR by comparing the results obtained with measured channels to those obtained with generic channel models both at the link and system levels. In contrast to most studies recently made available in the literature, this work is the first, to the best of our knowledge, to disclose realistic performance projections of a new enhanced transceiver technology for wireless networks beyond 3G with full synchronization (in time and frequency), channel identification and interference suppression capabilities.

II. DATA MODEL AND OVERVIEW OF STAR

A. Data Model

For the sake of simplicity, we consider the uplink direction of a cellular CDMA system where each base-station is equipped with M receiving antennas. We further consider a selective fading multipath environment characterized by P propagation paths where the time-delay spread $\Delta\tau$ is assumed small compared to T . The user’s BPSK symbol sequence is first differentially encoded at rate $1/T$ where T is the symbol duration. The resulting sequence $b(t)$ is then spread with a long personal PN code $c(t)$ at a rate $1/T_c$ where T_c is the chip pulse duration. The spreading factor is given by $L = T/T_c$.

After sampling at the chip rate and framing over $2L - 1$ chip samples at the symbol rate by the preprocessing unit, we obtain the $M \times (2L - 1)$ matched-filtering observation matrix:

$$\mathbf{Y}_n = [Y_n(0), Y_n(T_c), \dots, Y_n((2L - 2)T_c)] . \quad (1)$$

The structure of this matrix is detailed in [2]. After despreading \mathbf{Y}_n row-wise and framing the resulting post-correlation vector $Z(lT_c)$ over L chip samples at the

¹Work supported by a Canada Research Chair in High-Speed Wireless Communications and the Strategic Partnership Projects Program of NSERC.

symbol rate:

$$\mathbf{Z}_n = [Z_n(0), Z_n(T_c), \dots, Z_n((L-1)T_c)] , \quad (2)$$

we obtain the $M \times L$ -dimensional post-correlation observation matrix \mathbf{Z}_n [1]:

$$\mathbf{Z}_n = \underbrace{s_n \mathbf{H}_n}_{\text{ST channel}} + \mathbf{N}_n = s_n \underbrace{(\mathbf{J}_n \mathbf{D}_n^T)}_{\text{ST analysis}} + \mathbf{N}_n , \quad (3)$$

where $s_n = b_n \psi_n$ denotes the signal component, $b_n = b(nT)$ is the transmitted DBPSK symbol and ψ_n^2 is the total received power affected by the Doppler spread and multipath fading, the path-loss and shadowing and power control (PC). \mathbf{H}_n is the $M \times L$ spatio-temporal channel matrix. \mathbf{N}_n is the $M \times L$ spatio-temporal noise matrix after despreading with variance σ_N^2 . It includes the thermal noise received at the antenna elements as well as the self-, in-cell and out-cell interference. We hence define the input SNR after despreading as $SNR = \bar{\psi}^2 / \sigma_N^2$ where $\bar{\psi}^2$ denotes the average received power.

The most important feature in the equation above, referred to as the post-correlation model (PCM) in [1], is the spatial-temporal (ST) “analysis” of the channel matrix \mathbf{H}_n by its parametric decomposition, under structural constraints, as the the product of an $M \times P$ spatial channel matrix \mathbf{J}_n and a $P \times L$ temporal channel matrix \mathbf{D}_n^T . Indeed, $\mathbf{J}_n = \mathbf{G}_n \mathbf{Y}_n$ is itself the product of $\mathbf{G}_n = [G_{1,n}, \dots, G_{P,n}]$, the $M \times P$ column-wise normalized spatial channel matrix, and $\mathbf{Y}_n = \text{diag}[\varepsilon_{1,n}, \dots, \varepsilon_{P,n}]$, the $P \times P$ diagonal matrix of normalized power ratios over multipaths $\varepsilon_{p,n}^2$ (i.e., $\sum_{p=1}^P \varepsilon_{p,n}^2 = 1$). More importantly, each column of $\mathbf{D}_n = [D_{1,n}, \dots, D_{P,n}]$ belongs to a *temporal manifold*, i.e., its vector elements are known functions of a given parameter, namely the corresponding time-delay $\tau_{p,n}$ of the p -th multipath:

$$D_{p,n} = [\rho_c(-\tau_{p,n}), \dots, \rho_c((L-1)T_c - \tau_{p,n})]^T , \quad (4)$$

where $\rho_c(t)$ is a truncated raised-cosine pulse which corresponds to the correlation function of the square-root raised-cosine shaping-pulse $\phi(t)$.

B. Overview of STAR

The core idea of STAR is the following: A main channel estimation module, referred to as decision feedback identification (DFI) in [1], provides a coarse *unconstrained* estimate $\tilde{\mathbf{H}}_n$ of the spatio-temporal channel. In an analysis step, a space-time separation or decomposition of the channel follows by successive extraction of the temporal channel matrix $\hat{\mathbf{D}}_n$ (i.e., synchronization²) and the spatial channel matrix $\hat{\mathbf{J}}_n$. In a synthesis step, a space-time reconstruction of the channel then provides a far more accurate constrained estimate [1]:

$$\hat{\mathbf{H}}_n = \underbrace{\hat{\mathbf{J}}_n \hat{\mathbf{D}}_n^T}_{\text{ST channel synthesis}} = \hat{\mathbf{G}}_n \hat{\mathbf{Y}}_n \hat{\mathbf{D}}_n^T , \quad (5)$$

²The columns $\hat{D}_{p,n}$ are reconstructed using Eq. (4) after estimation of the multipath time-delays $\hat{\tau}_{p,n}$ and their number \hat{P} .

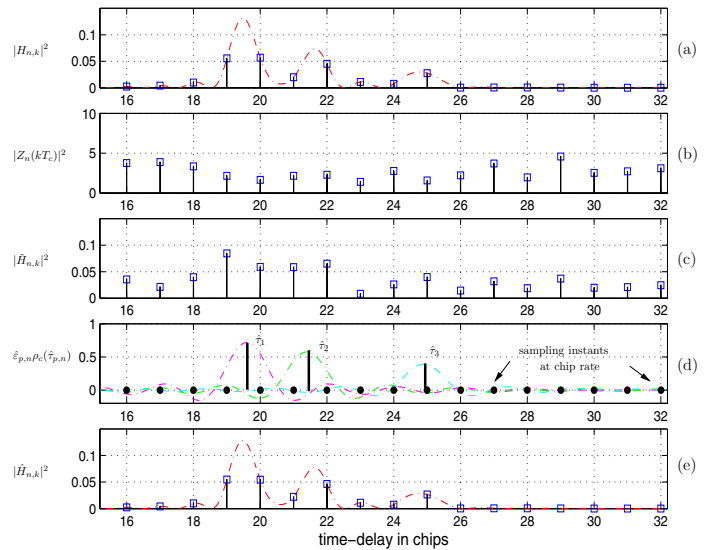


Fig. 1. Channel analysis/synthesis in STAR illustrated with $M = 1$ receive antenna: (a) power of chip-rate channel coefficients (power waveform is in dashed line), (b) power of chip-rate despreading observation, (c) power of unconstrained estimate of chip-rate channel coefficients, (d) channel analysis by high-resolution extraction from $\tilde{\mathbf{H}}_n$ of time-delays $\hat{\tau}_{p,n}$ and their number $\hat{P} = 3$, (e) power of constrained estimate of chip-rate channel coefficients after synthesis (resulting power waveform is in dashed line) by summation of $\hat{P} = 3$ replicas of a truncated raised-cosine pulse each delayed by $\hat{\tau}_{p,n}$ and weighted by $\hat{J}_{p,n} = \hat{\varepsilon}_{p,n} \hat{G}_{p,n}$, respectively, followed by chip-rate sampling.

by structure fitting along the nominal decomposition of the channel in Eqs. (3) and (4) of the PCM model. A final combining step exploits the *constrained* channel estimate $\hat{\mathbf{H}}_n$ to extract the signal component \hat{s}_n using simple MRC [2] or interference suppression [4]. Mathematical details can be found in [2], [4]. For simplicity here, we explain the concept and advantages of the analysis/synthesis-based design of STAR following the illustrations in Fig. 1.

The power of the spatio-temporal channel $\mathbf{H}_n = [H_{n,1}, \dots, H_{n,k}, \dots, H_{n,L}]$ is depicted in Fig. 1-a. It suggests that seven coefficients $H_{n,k}$, at least, have non-negligible power. In Fig. 1-b, the power of the despreading observation \mathbf{Z}_n of Eq. (2) shows that these seven most desired channel components are buried in noise. Conventional correlator-type receivers would average unmodulated post-correlation observations over time to bring these useful channel coefficients above a detection threshold. In contrast, the DFI module in STAR identifies the channel blindly using simple adaptive subspace tracking [1], [3]. As shown in Fig. 1-c, the resulting unconstrained estimate $\tilde{\mathbf{H}}_n = [\tilde{H}_{n,1}, \dots, \tilde{H}_{n,k}, \dots, \tilde{H}_{n,L}]$ constantly keeps the power of most of the desired channel components above the rest of the coefficients (which may sporadically exceed the detection threshold unnoticed [2]). Yet, it offers only a coarse estimate of the actual channel coefficients in Fig. 1-a.

It is at this stage that the analysis/synthesis design features contribute significantly to the enhanced performance

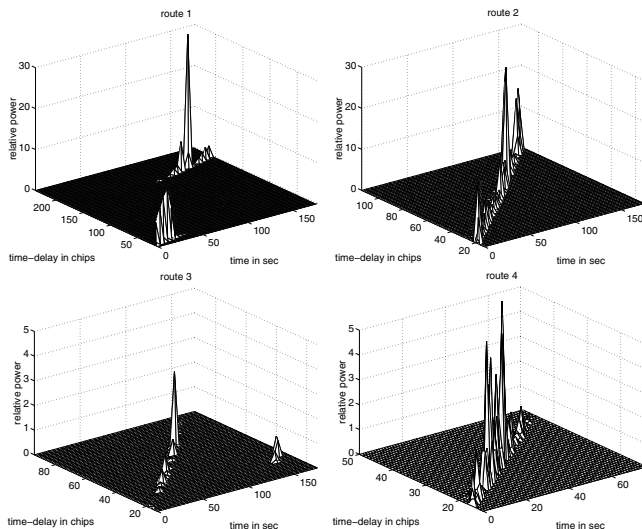


Fig. 2. Power vs. IR coefficient and time of the channel recordings collected along four different routes in Laval, a suburban area of Montreal, at vehicular speed below 30 Km/h (note synchronization hops in routes 1 and 3 due to channel sounder imperfections).

of STAR. Exploiting the parametric decomposition of the channel in Eqs. (3) and (4), STAR extracts by a high-resolution technique [1] the multipath time-delays $\hat{\tau}_{p,n}$ and their number \hat{P} from the unconstrained channel estimate $\hat{\mathbf{H}}_n$ depicted in Fig. 1-c. In Fig. 1-d, the multipath time-delays are accurately located with a resolution unlimited by the sampling rate or the clock precision. Estimation of the normalized multipath amplitudes $\hat{\varepsilon}_{p,n}$ and the complex fading components $\hat{G}_{p,n}$ completes the analysis step and allows for reconstruction of the constrained channel estimate $\hat{\mathbf{H}}_n = [\hat{H}_{n,1}, \dots, \hat{H}_{n,k}, \dots, \hat{H}_{n,L}]$ in the synthesis step. In Fig. 1-e, the resulting enhanced channel estimate is the best constrained fit that can be extracted from the unconstrained estimate $\hat{\mathbf{H}}_n$ depicted in Fig. 1-c.

III. REAL-WORLD DATABASE AND SIMULATOR SETUP

A. Real-World Database

A database of real-world radio-channel measurements was recently made available for this study by Rogers Wireless. The database contains, in a raw format, impulse response (IR) measurements of 5 MHz radio-channels recorded between a roof-top transmit antenna and a single receive antenna (*i.e.*, $M = 1$) mounted inside a mobile mini-van. The channel sounder was operated in the North American PCS band at a carrier frequency of 1982.5 MHz by continuously transmitting an unmodulated PN-sequence of 255 chips at the former WCDMA chip-rate of 4.096 Mcps (which still serves the purpose of this evaluation work). After capturing the off-air signal via a wideband mono-pole antenna, the received signal was successively passed through a pre-selector filter, a low noise amplifier (LNA), an image reject filter followed by a single-conversion quadrature down-converter. The I and Q components were sampled at a rate of 8.192 MHz (oversampling by a factor of 2) using a 12 bit-resolution A/D for

| Parameter | Value | Comment |
|-------------------|---------------|-----------------------------|
| f_c | 1.9825 GHz | carrier frequency |
| R_c | 4.096 Mcps | chip rate |
| R_b | 8/256 Kb/s | bit rate |
| r | 1/2 | coding rate |
| K | 9 | constraint length |
| M | 1 | number of antennas |
| L | 256/8 | spreading factor |
| $L_{\Delta} = 32$ | 32 chips | reduced processing window |
| β | 0.22 | RRC rolloff factor |
| N_c | 17 | number of RRC coefficients |
| f_{PC} | 1600 Hz | frequency of PC updating |
| ΔP_{PC} | ± 0.25 dB | PC adjustment |
| τ_{PC} | 0.625 ms | PC feedback delay |
| BER_{PC} | 5% | simulated PC bit error rate |

TABLE I
Parameters used in the simulations.

each output. Note, however, that STAR does not require oversampling and will only exploit the measurements at the chip-rate. Each quadrature signal was acquired every 1 msec and was continuously streamed to the disk. Full details of the recording setup and conditions are provided in [9].

From this database, we have been able to exploit four IR recordings conducted at the so-called site 132 in Laval (a suburban area of Montreal) [9]. They correspond to four different routes of the mini-van close to a mall in the suburban Laval area (*i.e.*, site 132), all long enough to allow for a reliable performance verification.

B. Simulator Setup

The simulator is composed of a link-level module and a system-level one. The link-level module integrates STAR in a transceiver structure that includes a channel coder, an interleaver, a spreader and a power amplifier at the transmitter, a baseband multipath Rayleigh-fading³ channel generator, an additive interference generator, a despreader, the STAR receiver, a deinterleaver, a channel decoder and a power control (PC) unit at the receiver. The parameters used by the simulator are reported in Tab. I (unless specified otherwise). For a specified input SNR level, the simulator provides link-level statistics such as the symbol error rate (SER) or frame error rate (FER) as well as transmit and receive power distributions. The system-level module uniformly populates a square grid of cells with a total number of users and measures the total received interference at the base-station of the central cell taking into account the transmit and receive power distributions. For a specified capacity C defined as the average number of users per cell, it provides the outage probability that the signal to interference ratio is below a given input SNR [2].

The baseband channel generator operates with both generic models and IR measurements directly fed to the

³Study of the measurements did not reveal line-of-sight components typical of Ricean channels.

| | | rte 1 | rte 2 | rte 3 | rte 4 |
|--|----------------------|-------|-------|-------|-------|
| P_t [%] | 1 st path | 100 | 100 | 100 | 100 |
| | 2 nd path | 99 | 97 | 99 | 99 |
| | 3 rd path | 71 | 60 | 85 | 48 |
| $\widehat{d\tau}$ [ppm] | | 0.10 | 0.14 | 0.12 | 0.10 |
| $\frac{\varepsilon_p^2}{\varepsilon_1^2}$ [dB] | 1 st path | 0 | 0 | 0 | 0 |
| | 2 nd path | -3.9 | -4.3 | -3.8 | -4.3 |
| | 3 rd path | -7.8 | -8.0 | -7.7 | -7.7 |
| $\overline{\Delta f}$ [Hz] | | 179 | 61 | 89 | 120 |
| $\widehat{f_D}$ [Hz] | | 42 | 30 | 41 | 10 |
| \widehat{v}_{\max} [Km/h] | | 23 | 17 | 22 | 6 |

TABLE II

Multipath extraction percentage over time P_t and extracted channel parameters from data (delay drift $\widehat{d\tau}$, average multipath power profile $\frac{\varepsilon_p^2}{\varepsilon_1^2}$, carrier frequency offset $\overline{\Delta f}$, maximum Doppler spread $\widehat{f_D}$ or speed \widehat{v}_{\max}).

link-level module. In a preliminary dynamic channel characterization phase [7], only the link-level module is used and the channel generator there is operated with the IR measurements noise-free for the sole purpose of extracting the channel parameters. For performance verification, both simulator modules are first operated with generic channels tuned by the parameters extracted in the preliminary dynamic characterization phase, then with the measured channels.

IV. RECEIVER PERFORMANCE EVALUATION RESULTS

A. Extracted Channel Parameters

STAR takes advantage of its powerful channel parameter extraction capability based on the “analysis/synthesis” principle (*cf.* section II-B) to provide a new dynamic characterization of wideband radio channels (*i.e.*, extraction and modeling of time-evolution profiles of time-delays, CFO, Doppler spread, etc. . .), so essential to an adaptive receiver for online adjustment to changing propagation conditions. For lack of space, we refer the reader to [7] for full details. In Tab. II, we report only the extracted channel parameters needed for the tuning of the simulator (*cf.* section III-B). Note, however, that we use the same average multipath power profile of [0, -4, -8] dB for simplicity. Furthermore, we set the initial multipath time-delays to [10, 12, 14] T_c before linear drift and set both the CFO and speed to be constant.

B. Voice Rate

In this section, we verify the performance of STAR at both the link-level in terms of BER vs. SNR in Fig. 3, and the system-level in terms of maximum capacity (in users per cell) at 1% outage and 10^{-3} BER in Tab. III, by comparing the results obtained with measured channels and those obtained with the generic ones. The BER curves in Fig. 3 and the required SNR thresholds in Tab. III do not indicate any particular ordering in performance linked

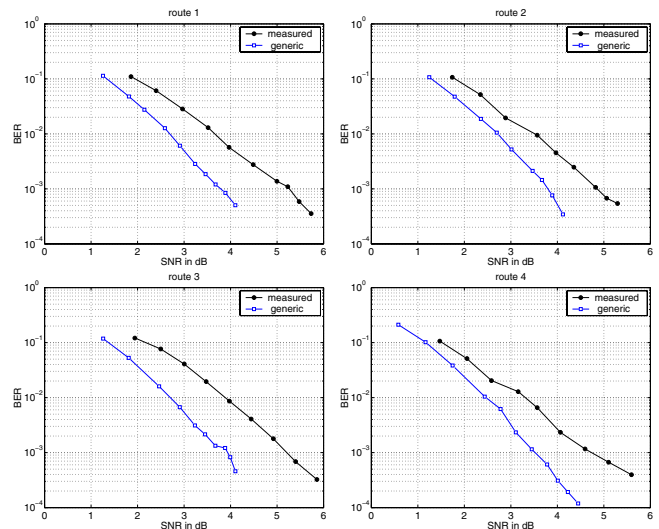


Fig. 3. Link-level performance of STAR at 8 Kb/s for both measured and generic channels: BER vs. input SNR with one receive antenna.

to the variations of a specific channel parameter in Tab. II. More importantly, they show a constant gap of about 1.0 to 1.3 dB between the measured and generic channels resulting in 20 to 30% losses in capacity, regardless of the route. This is consistent with the fact that performance was optimized over all the design dimensions of STAR made available by analysis/synthesis of the channel, *i.e.*, in terms of timing (time-delay parameter), CFO (CFO parameter) and adaptive channel identification (multipath component and speed parameters). We attribute the mismatch of about 1 dB to other common sources of imperfection not taken into account in the generic channels. There are potentially many in practice: non-linear multiplicative noise, shaping-filter distortions, adaptive gain control (AGC) errors and power amplifier saturation, etc. . . which all contribute to power leakage from the desired signal. There are very good reasons to believe that the experimental channel sounder used by Rogers Wireless for the channel measurements suffers from large amounts of such design imperfections (*cf.* caption of Fig. 2 as an example). Promising to note, though, that such imperfection levels are unlikely in commercial wireless products. Lower SNR gaps and capacity losses could therefore be expected in practice. With the tested data, STAR (without a pilot, *i.e.*, blind) would still accommodate about 45 DBPSK users per cell or sector at 8 Kb/s, thereby offering a potential spectrum efficiency of about 0.09 bps/Hz over measured channels with single transmit and receive antennas only.

C. High Data-Rate (HDR)

To verify the performance at higher data rates, we additionally considered the assessment of a HDR configuration of STAR at 512 Kb/s before channel decoding (*i.e.*, spreading factor $L = 8$). To do so, we used the block-structured HDR implementation of STAR proposed in [10] with a processing block length of 256 chips (see details in [10]). Since reliable BER accuracy below 10^{-6} could

| Channel | route 1 | | route 2 | | route 3 | | route 4 | |
|----------|---------------------|---------------------------------|---------------------|---------------------------------|---------------------|---------------------------------|---------------------|---------------------------------|
| | SNR_{req} [dB] | C_{max} [users p. cell] |
| Measured | 5.2 | 43 | 4.8 | 45 | 5.2 | 43 | 4.7 | 48 |
| Generic | 3.9 | 63 | 3.8 | 63 | 4.0 | 58 | 3.6 | 64 |
| Mismatch | 1.3 | 31% | 1.0 | 28% | 1.2 | 22% | 1.1 | 25% |

TABLE III

System-level performance of STAR at 8 Kb/s for both measured and generic channels: required SNR at 10^{-3} BER and corresponding capacity at 1% outage with one receive antenna.

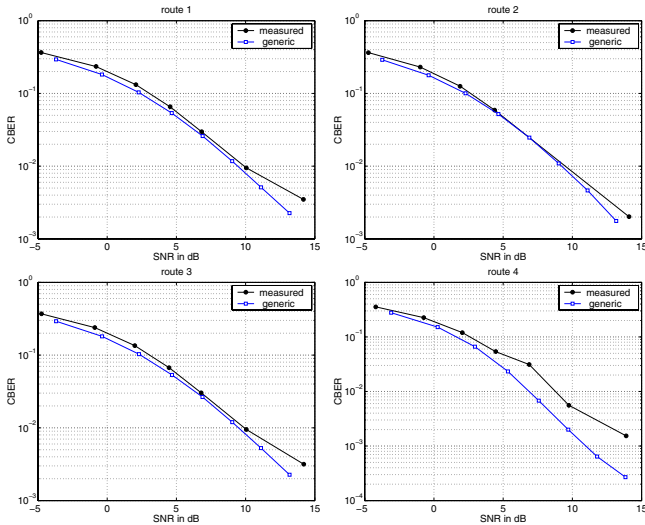


Fig. 4. Link-level performance of STAR at 512 Kb/s (*i.e.*, 256 Kb/s assuming rate-1/2 channel coding) for both measured and generic channels: CBER (coded BER, *i.e.*, BER before channel decoding) vs. input SNR with one receive antenna.

not be achieved with the available data and simulation time increases significantly with the data rate, we limited the performance verification to the link-level only. System-level capacity results at this high rate will be considered in the next section along with the multi-user detection upgrade of STAR. Simulation results in terms of BER curves before channel decoding vs. SNR in Fig. 4 suggest that STAR works equally well at 512 Kb/s over measured channels and that the SNR gap, assuming a target BER of 10% before channel decoding, is again in the range of 1 dB between measured and generic channels. This result is consistent with the observation made above on the impact of imperfection sources on performance as a main mismatch/loss factor.

D. HDR with Multi-User Detection Upgrade

Multi-user detection and interference suppression are most effective for capacity enhancement at high data rates. Recently we proposed a new interference subspace rejection (ISR) paradigm [4] as an upgrade of the simple MRC combiner of STAR. More recently, the resulting STAR-ISR receiver was found to outperform the RAKE-PIC (parallel interference canceller) by factor 4 to 7 in spectrum efficiency [10]. Here we further pushed the per-

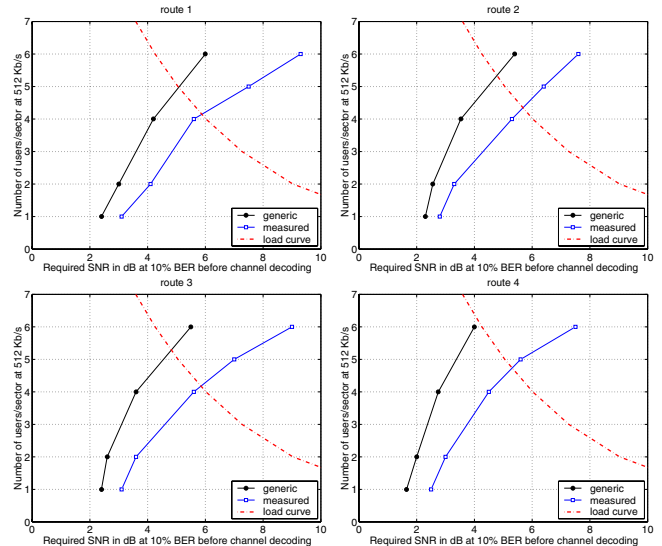


Fig. 5. Link-level performance of STAR-ISR at 512 Kb/s (*i.e.*, 256 Kb/s assuming rate-1/2 channel coding) for both measured and generic channels: required SNR at 10^{-1} BER (before channel decoding) vs. the number of in-cell users per cell (or sector) targeted for suppression with one receive antenna (the load curve for an out-cell to in-cell interference ratio $f_{O/I} = 0.6$ is in dashed line).

formance verification stage to the assessment of STAR-ISR at 512 Kb/s over measured channels. To do so, we modified the link-level module to include multiple access interference from a given number of in-cell (or in-sector) users as well as an equal number of STAR-ISR receivers dedicated each to the detection of one different user and to the suppression of the others. For each route, we sliced the corresponding channel recording into a similar number of far-spaced segments with equal durations. Each portion represents a shorter but quasi-independent channel of a different in-cell (or in-sector) user, taken however from the same route to keep the channel conditions identical for simplicity (*i.e.*, the generic channels are tuned with the same set of parameters). In Fig. 5, the link-level simulation results in terms of required SNR at 10% BER before channel decoding vs. the number of in-cell (or in-sector) users suggest that the gap between the generic and measured channels keeps widening beyond the 1 dB range reported previously in the single-user case (*i.e.*, the two lowest SNR points). With 6 users, the SNR gap is between 2 and 3.5 dB. We attribute this widening gap to the larger

| Channel | route 1 | | route 2 | | route 3 | | route 4 | |
|----------|---------------------|-------------------------------|---------------------|-------------------------------|---------------------|-------------------------------|---------------------|-------------------------------|
| | SNR_{req} [dB] | C_{max} users p. cell |
| Measured | 5.6 | 4 | 5.4 | 4 | 5.7 | 4 | 4.6 | 4 |
| Generic | 5.0 | 5 | 4.4 | 5 | 4.7 | 5 | 4.0 | 6 |
| Mismatch | 0.6 | 20% | 1.0 | 20% | 1.0 | 20% | 0.6 | 33% |

TABLE IV

System-level performance of STAR-ISR at 512 Kb/s for both measured and generic channels: required SNR at 10^{-1} BER (before channel decoding) and corresponding capacity with one receive antenna.

impact of imperfections (not taken into account in the generic channels) on the reconstruction and suppression of increasing amounts of interference signals. In any case, however, it is very important to report on the gap between the required SNR values at maximum achievable capacity for both the generic and measured channels. In Tab. IV of system-level results, we provide these SNR values along with the corresponding maximum capacities achievable below the dashed-line load curve in Fig. 5 for an out-cell to in-cell interference ratio $f_{O/I} = 0.6$ [11]. As in the voice-rate single-user case (*cf.* sec IV-B), the SNR gap is in the range of 1 dB and results in 20 to 30% losses in capacity. Yet, STAR-ISR (without a pilot, *i.e.*, blind) would still accommodate 4 DBPSK users per cell or sector at 256 Kb/s (assuming rate-1/2 channel coding), thereby offering a potential spectrum efficiency of 0.25 bps/Hz over measured channels with single transmit and receive antennas only.

E. Discussion

In both cases of voice-rate single-user STAR and HDR MUD STAR-ISR, imperfections not taken into account when using generic channels result in consistent shifts in required SNR of about 1 dB. Although the associated capacity losses of 20 to 30% are significant, we still consider the performance achieved as promising bearing in mind the fact that the experimental channel sounder used to collect the data does not match the accuracy of commercial wireless terminals. Lower losses in SNR performance could be anticipated in a prospective integration of STAR (or STAR-ISR) in wireless terminals.

Significant challenges remain, however, in verifying by means of field experiments with multiple moving transmitters and/or receivers the performance results obtained by simulation of the radio propagation environment. We are currently building a prototype of STAR to validate it in real time and “over the air”. We have already laid out a preliminary architecture for STAR [8], [12] based on hardware/software codesign.

V. CONCLUSIONS

In this work, we verified the performance of STAR by comparing the results achieved with generic and measured channels for an average multipath power profile of [0, -4, -8] dB and a vehicular speed of 30 Km/h. With one transmit

and one receive antenna only, results suggest that losses in SNR and capacity due to operation of STAR (without a pilot, *i.e.*, blind) over measured 5 MHz channels are in the range of 1 dB and 20-30%, respectively, with DBPSK. The required SNR threshold for receiver operation over measured channels is near 5 dB. This corresponds to a spectrum efficiency of about 0.09 bps/Hz at 8 Kb/s, and 0.25 bps/Hz at 256 Kb/s with a multi-user detection upgrade of STAR.

REFERENCES

- [1] S. Affes and P. Mermelstein, “A new receiver structure for asynchronous CDMA: STAR - the spatio-temporal array-receiver,” *IEEE J. Select. Areas in Commun.*, vol. 16, no. 8, pp. 1411–1422, Oct. 1998.
- [2] K. Cheikhrouhou, S. Affes, and P. Mermelstein, “Impact of synchronization on performance of enhanced array-receivers in wideband CDMA networks,” *IEEE J. Select. Areas in Commun.*, vol. 19, no. 12, pp. 2462–2476, Dec. 2001.
- [3] S. Affes and P. Mermelstein, “Adaptive space-time processing for wireless CDMA,” in *Adaptive Signal Processing: Application to Real-World Problems*, J. Benesty and Y. Huang, Eds. Berlin: Springer, Jan. 2003, ch. 10.
- [4] S. Affes, H. Hansen, and P. Mermelstein, “Interference subspace rejection: A framework for multiuser detection in wideband CDMA,” *IEEE J. Select. Areas in Commun.*, vol. 20, no. 2, pp. 287–302, Feb. 2002.
- [5] B. Smida, S. Affes, and P. Mermelstein, “Joint time-delay and frequency offset synchronization for CDMA array-receivers,” in *Proc. of IEEE SPAWC’03*, Rome, Italy, Jun. 2003, pp. 499–504.
- [6] H. Hansen, S. Affes, and P. Mermelstein, “High capacity downlink transmission with MIMO interference subspace rejection in multicellular CDMA networks,” *EURASIP J. App. Sig. Proces.*, vol. 2004, no. 5, pp. 707–726, May 2004.
- [7] K. Cheikhrouhou, S. Affes, A. Elderini, B. Smida, P. Mermelstein, B. Sultana, and V. Sampath, “Design verification and performance evaluation of an enhanced wideband CDMA receiver using channel measurements,” *EURASIP J. App. Sig. Proces.*, no. 11, pp. 1736–1752, Jul. 2005.
- [8] S. Jomphe, J. Belzile, S. Affes, and K. Cheikhrouhou, “Codesign implementation of a 3G WCDMA base station receiver,” in *Proc. of IEEE CCECE’04*, May 2004, pp. 1191–1194.
- [9] S. Aridhi *et al.*, “Third generation trial, final report - phase 1,” Microcell Connexions, Montreal, Tech. Rep., Mar. 1999.
- [10] S. Affes, K. Cheikhrouhou, and P. Mermelstein, “Enhanced interference suppression for spectrum-efficient high data-rate transmissions over wideband CDMA networks,” in *Proc. of IEEE ICASSP’03*, vol. IV, Apr. 2003, pp. 469–472.
- [11] A. Viterbi, *CDMA Principles of Spread Spectrum Communication*. Addison-Wesley, 1995.
- [12] S. Jomphe, “Réalisation et validation en VHDL d’un récepteur de station de base à modulation en étalement de spectre,” Master’s thesis, ÉTS, 2005.